JOURNAL OF MATERIALS SCIENCE 31 (1996) 3813–3819

Effects of hydrostatic extrusion on the mechanical and thermal properties of polypropylene

T. ARIYAMA
Department of Mechanical Engineering, Faculty of Engineering, Science University of Tokyo, 1-3 Kagurazaka, Shinjuku-ku, Tokyo 162, Japan

The structure change in spherulites for hydrostatically extruded polypropylene (PP) was studied by the use of internal friction measurements and thermophotometry tests. The onset temperature of the β-loss peak of the PP sample decreases with increasing reduction in area, R. For the extrudates below $R=50\%$, the peak temperature of α-loss shifts to lower temperature. The α and β absorptions for the extrudates up to $R=50\%$ become broad and overlap with each other. The intensity of the β-loss peak, Δ_{max}, is maximum for the extrudate with $R=50\%$. The results of tan δ, damping, and the intensity of the β-loss peak indicate that the mechanism of molecular chain deformation is divided into two stages, below and above $R=50\%$. The results are due to spherulitic changes, i.e. the shape of spherulites changed from spherical to elliptical in the extrudates above $R=50\%$ and the spherulite with $R=50\%$ changed from coarse structure to a finer one by the imposition of hydrostatic pressure.

1. Introduction

A considerable number of studies have been performed on the effects of hydrostatic pressure on polymers [1]. The primary interest in applying the techniques of hydrostatic extrusion to the deformation processing of polymer is in improving the mechanical properties of the material. The solid-phase hydrostatic extrusion of thermoplastics at room temperature has been investigated by Pugh and Low [2]. Much research has been conducted on the hydrostatic extrusion of polyethylene and resulting properties of the extrudates [3–13]. Structural changes in polyethylene extrudates give rise to a higher tensile modulus and a higher degree of orientation with increasing extrusion ratio.

Some investigators [14–20] have studied the hydrostatic extrusion of PP and properties of extrudates at various temperatures. Buckley and Long [14] studied the effect of extrusion ratio (up to 5.4) on torsional modulus, density, and melting point, along with wide-angle X-ray diffraction analysis, and concluded that there is no appreciable change in density and melting points. Williams [15] studied the effect of deformation ratio (up to 15) on the tensile and torsional moduli of polypropylene (PP) extrudates when hydrostatically extruded at 100 °C. He reported the tensile modulus of the extrudate increased with increase in the extrusion ratio, and indicated from both birefringence and X-ray diffraction that deformation is non-affine. Yoon *et al.* [16] showed from X-ray analysis of PP extrudates that c-axis orientation of the polymer chains occurred and the extent of the orientation was enhanced with an increase in extrusion ratio. Similar changes in X-ray patterns occurred at high extrusion ratios and the Vickers' hardness number of extrudates depended on the crystalline orientation and the crystallinity [17, 18].

The melting point, specific heat, and morphology of hydrostatically extruded PP have been studied to clarify the plastic deformation of three different parts of the extrudates (pheriphery, intermediate, and core) parallel to the direction of hydrostatic extrusion [20]. Differential scanning calorimeter (DSC) measurements showed that, for all the parts studied, the peak and the end-of-transition temperatures had a minimum value at a percentage reduction in area, R, of 50%. Similar behaviour was observed for the specific heat evaluated at several temperatures below the melting point. The morphological structure observed by use of a polarizing microscope indicated that the shape of spherulites above $R = 50\%$ changed from spherulitic to elliptical. The pronounced changes taking place around $R = 50\%$ are closely related to the marked bend in the extrusion pressure versus extrusion ratio curve which takes place at the same R value.

The glass transition temperature, T_g, has been studied for hydrostatically extruded polycarbonate (PC) [21]. The T_g behaviour of the PC extrudates with $R = 40$–50% changed markedly in DSC curve shape in contrast to the as-received PC. The peak temperature of the PC extrudates changed in the same manner as the T_g behaviour. These facts suggested that the stiff phenylpropane groups were deformed by the imposition of hydrostatic extrusion. The hydrostatic extrusion of the PC billet showed that a

0022–2461

two-stage deformation process of the molecular chains might occur and that an R value of 50% might be a kind of critical value.

Shear-banding was observed for high-impact polystyrene (HIPS) extrudates with $R = 30$–60%; this fact indicated that a sub-glass transition (β-transition) occurred in the temperature range below T_g [21]. The appearance of a β-transition was caused by the imposition of hydrostatic extrusion. On the contrary, the T_g behaviour and the transparency of the HIPS extrudate with $R = 70\%$ suggested that this billet had been hydrostatically extruded under the restriction of the motion of phenyl groups. The molecular chains of HIPS extrudates with $R = 70\%$ might be oriented in the direction of hydrostatic extrusion. The peak temperature for the HIPS with $R = 70\%$ closely agreed with that of isotactic polystyrene having about 70% tacticity calculated from infrared spectra [22].

A study was also made of the thermal properties of hydrostatically extruded polymers of poly(methyl methacrylate) extrusions (PMMA-ext). The essential results of the experimental study were that the T_g of the PMMA-ext extrudate with $R = 50\%$ was about 10 °C lower than the as-received sample, and that the decomposition temperature increased with increasing reduction in area but, after passing through a maximum increase of 30 °C at $R = 50\%$, it started to decrease and returned to its starting value of about 223 °C at $R = 70\%$ [22]. The observed effects of hydrostatic extrusion on the thermal properties of the amorphous polymers, PMMA-ext and HIPS, agreed well with that on the mechanical behaviour, which was reported elsewhere [17, 18].

Hydrostatic extrusion of polymers, which is still at the basic research and development stage, has considerable merits; higher elastic modulus, yield or fracture stress, and, in some cases, higher elongation at fracture of the resulting extrudates are only a few of the advantages of this process [17, 18]. On the contrary, the hydrostatic extrusion of metals and ceramics has been established as an industrial process [23–25]. In the present study, the effect of hydrostatic pressure on the molecular deformation of PP samples extended under hydrostatic pressure was investigated using internal friction measurements and thermophotometry tests. The results are discussed on the basis of spherulitic structure to clarify the structural change of hydrostatically extruded PP.

2. Experimental procedure

2.1. Materials

The rod-like polypropylene (PP, Ube Industries, Ltd, Grade J105) was used: crystal modification was the monoclinic α-form and the melt flow index was 0.005 kg/10 min (temperature = 230 °C and force = 1.54 MPa). The material had an apparent density of 907 kg m^{-3}. The degree of crystallinity calculated from the density was 56%, where values of 870 kg m^{-3} for completely amorphous density and of 936 kg m^{-3} for crystalline density were used [26]. The number-average molecular weight was 285 000, which was estimated from the melt flow index. The mean spherulite diameter of the materials was 180 μm [20]. Materials were machined to nosed billets with adequate diameter for various reductions in cross-sectional area, R, up to $R = 80\%$: $R(\%) = 100[1 - (d/D)]^2$, where d is the die outlet diameter of 9 mm, and D the original billet diameter. The microstructure of the cross-section of the billets was homogeneous: this was confirmed from an observation of the spherulitic morphology using polarizing microscopy [20]. The billets were hydrostatically extruded by a high-pressure apparatus, with castor oil as a pressure medium, under hydrostatic pressure up to 120 MPa. The semicone angle of the die was chosen to be 20° and the extrusion rate at the die exit was 5.3 mm s^{-1}. A detailed description of the extrusion procedure is given elsewhere [27].

2.2. Measurement of internal friction

A counter-suspension type torsion pendulum apparatus was used to measure the internal friction. A detailed description of the internal friction measurements and the quantitative evaluation of the internal friction can be found elsewhere [23, 24]. Torsion pendulum measurements were made at approximately 1 Hz over the temperature range −120 to 100 °C. Samples were cut to give test pieces of dimensions 25 mm by 2 mm by 2 mm and the distance between the sample holders was kept at 15 mm for all tests. The measurements were carried out under dried nitrogen at a heating rate of 1 °C min^{-1}.

2.3. Thermophotometry tests

Thermophotometry (TP) tests with the improvement of a polarizing microscope, were performed for PP extrudates to investigate the melting behaviour. The change in the intensity of light transmitted through a thin section of the samples was detected by means of a CdS cell. A hot stage was set on a revolving stage of the polarizing microscope. The sample was placed directly on the heater composed of an electroconductive glass, which was coated with tin and metallic oxide. The TP tests were carried at a heating rate of 2 °C min^{-1}. The details of the device for the TP tests can be found elsewhere [25]. Film about 10 μm thick was microtomed at various cutting angles of $\theta = 0$ and $\pi/2$ rad to the extrusion direction.

3. Results and discussion

3.1. Torsional dynamic mechanical properties

Fig. 1 shows the temperature dependence of tan δ (loss factor) of PP extrudates with various reductions in area, R, together with the virgin sample. Two separate peaks are observed for the virgin sample over the temperature range tested here: the peak occurring at about 5 °C, the β-loss peak, is attributed to the glass–rubber transition of the amorphous phase [28, 29], and the peak appearing around 75 °C is associated with the α absorption of the crystalline phase [30]. Tan δ curves for the extrudates show

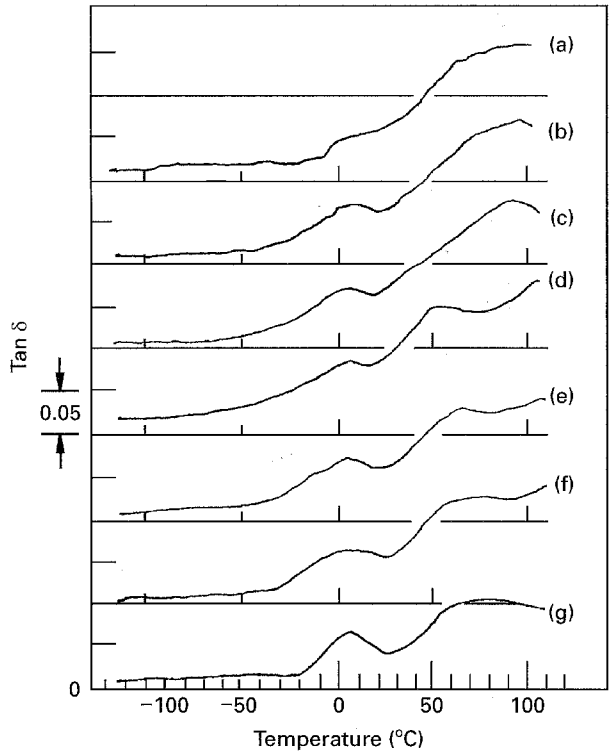

Figure 1 Tan δ versus temperature of PP extrudates with different reductions in area R: (a) 80%; (b) 70%; (c) 60%; (d) 50%; (e) 40%; (f) 30%; (g) virgin sample. Curves are shifted vertically for clarity.

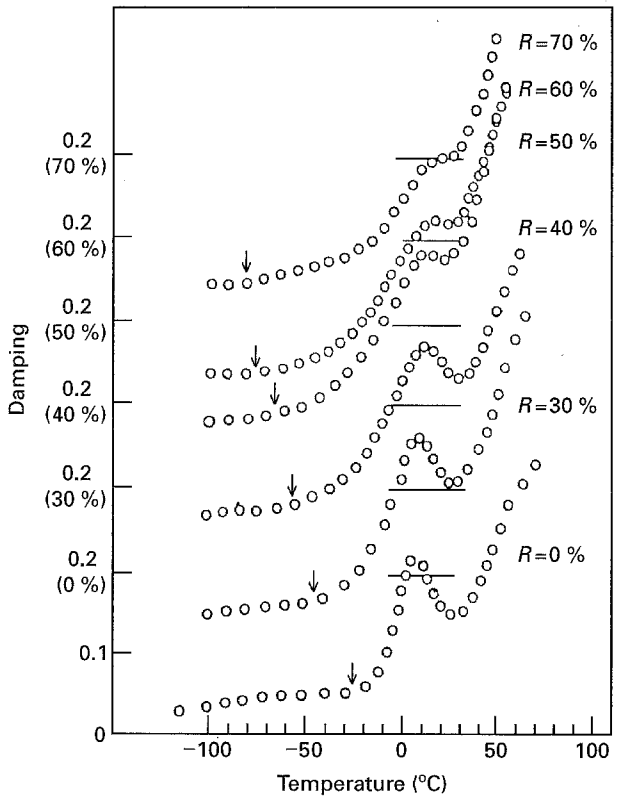

Figure 2 Temperature dependence of damping of PP extrudates with different reductions in area R. Curves are shifted vertically for clarity.

complicated features. Fig. 2 shows the damping versus temperature of the PP extrudates and the virgin sample. The onset temperature of the β-loss peak is indicated by allows in Fig. 2 and the results of the onset temperature are shown in Fig. 3. The onset

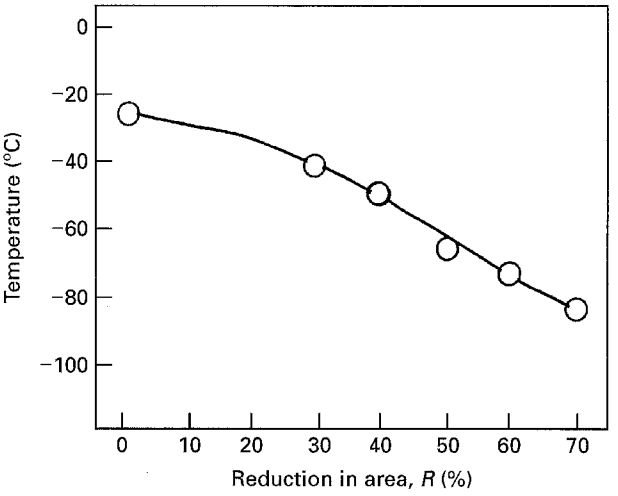

Figure 3 Onset temperature of the β-loss peak versus reduction in area of PP extrudates.

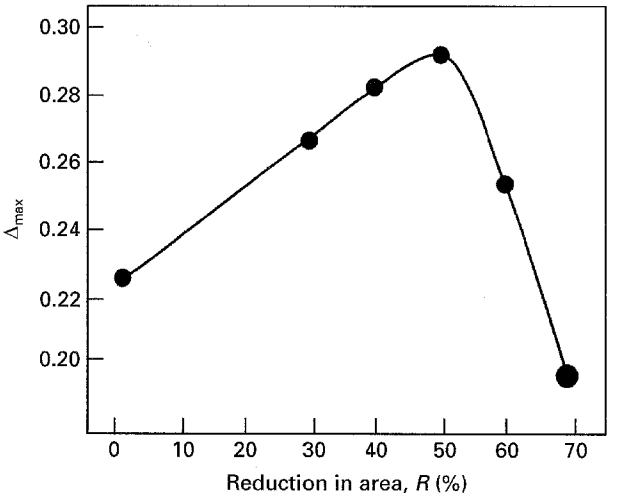

Figure 4 Intensity of the β-loss peak, Δ_{max}, versus reduction in area of PP extrudates.

temperature decreases with increasing reduction in area, R. For the extrudates below $R = 50\%$, both the onset temperature of β-loss and the peak temperature of α-loss, shift to lower temperature. In addition, the α and β absorptions for the extrudates up to $R = 50\%$ become broad and overlap with each other. For the extrudates above $R = 50\%$, the α absorption shifts to the higher temperature, in contrast to the curve behaviour of the reduction in area below $R = 50\%$. It is noticed that the temperature of the β-loss peaks does not shift and remains constant at 5 °C. It is reported [28, 29] that the glass transition temperature, T_g, of PP is −18 °C: this T_g value agrees with the onset temperature of the virgin sample. The α relaxation is attributed to molecular motion due to diffusion within the crystalline phase [30]. These β- and α-loss peaks in the virgin sample are clearly separated.

Fig. 4 shows the intensity of the β-loss peak, Δ_{max}, versus the reduction in area, R. The intensity is maximum for the extrudate with $R = 50\%$. The results of tan δ, damping, and the intensity of the β-loss peak indicate that the mechanism of molecular chain deformation is divided into two stages: (a) below and (b) above $R = 50\%$.

3.1.1. Molecular chain deformation below $R = 50\%$

The results of direct observations of polarizing micrographs for PP extrudates have shown that the size of spherulites or the mean diameter of spherulites decreased with increasing reduction in area up to $R = 50\%$: i.e. during the course of hydrostatic extrusion below $R = 50\%$, it appears that the coarse spherulites, which existed in the virgin sample, were crushed to fine spherulites by the hydrostatic extrusion. In addition, the degree of crystallinity determined by the apparent density decreased with increasing reduction in area up to $R = 50\%$ [17, 18]. From these experimental results, the increase in β-loss peak intensity is due to the increase in amorphous molecules squeezed from the interior of spherulites by hydrostatic extrusion. This is because the location of the onset temperature for the β-loss peak shifts to lower temperature as the reduction in area increases, as shown in Fig. 3.

3.1.2. Molecular chain deformation above $R = 50\%$

The α absorption for the extrudates above $R = 50\%$ differs from that of the virgin sample: the α-peak temperature for the extrudates is higher by about 20 °C than that for the virgin sample. In addition, the morphological structure observed by use of a polarizing microscope indicated that the shape of spherulites above $R = 50\%$ changed from spherulitic to elliptical [20]. The overlap of α- and β-losses is due to molecular chains strained on hydrostatic extrusion.

3.2. Comparison with a cold-drawn sample

Fig. 5 shows the torsional modulus G' versus temperature for the PP extrudate with $R = 80\%$, the cold-drawn PP with a draw ratio of $\lambda = 5$, and the PP virgin sample. In the three samples, the α- and β-loss peaks became broad and overlapped with each other and the intensities of the α-loss peak were larger than those of the virgin sample. This behaviour may be attributed to the structural reorganization of molecular chains produced by extrusion operation. In the cold-drawn sample, the molecular chains were oriented to the extension direction and formed into a fibrillar structure. In the extruded sample, with $R = 80\%$, the spherulites were deformed from a spherulitic to a elliptical (or an egg-shaped) character in the direction of the deformation [20]. The torsional modulus, G', for the extrudates below $R = 50\%$ and the virgin sample, decreases gradually above 25 °C. For the extrudate with $R = 80\%$ (H in Fig. 5), however, the G' curve exhibits a bilinear fashion above 25 °C and a break in the curve occurs at around 70 °C.

3.3. Analysis of the β-loss peak and period

Fig. 6 shows the damping and period versus temperature for the core part of the extrudate with $R = 30\%$. The β- and α-loss peaks in the virgin sample are clearly separated, as shown in Fig. 1. For the various extrudates up to $R = 80\%$, however, the damping curve indicates complicated behavior: i.e. the β- and α-loss peaks are overlapped each other (Fig. 6). To analyse the β-loss peak, the peak value A is introduced: i.e. the peak value A is defined as the damping value obtained by subtracting the damping value of the base line from the magnitude of the β-loss peak. The results are given in Fig. 7 as a function of reduction in area. The peak value A decreases with increasing reduction in area. In particular, the steep decrease in the value A is observed at the reduction in area of $R = 40$–50%. This fact is due to the change of chain deformation, i.e. the morphological structure indicated that the shape of spherulites above $R = 50\%$ changed from spherulitic to elliptical [20].

The time of existence of the core part of extrudate with $R = 30\%$ gradually increases as reduction in area increases (Fig. 6). The same behaviour of this period is observed in other parts (periphery and intermediate) of various extrudates up to $R = 80\%$. Below a temperature of 0 °C, the time is less than 1 s, but above 0 °C, the slope of the period becomes steeper. This may be attributed to the molecular change by the imposition of hydrostatic extrusion. The torsional

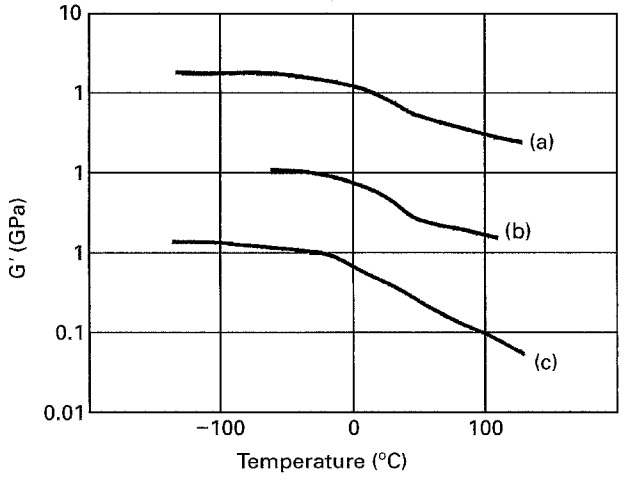

Figure 5 Torsional modulus G' versus temperature of different PP samples: (a) cold-drawn sample with draw ratio $\lambda = 5$; (b) extrudate with $R = 80\%$; (c) virgin sample.

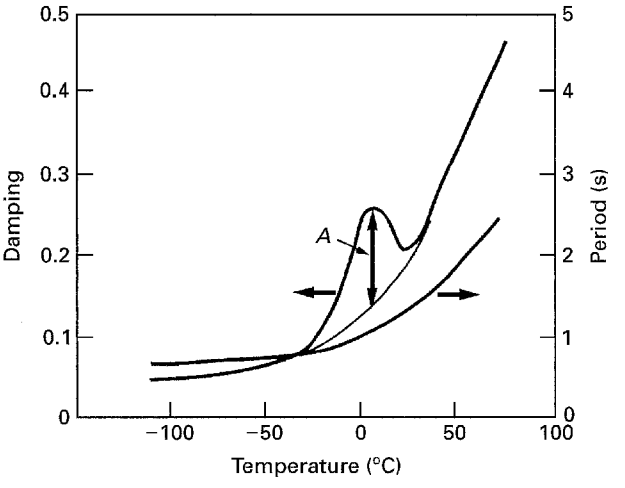

Figure 6 Damping and period versus temperature of a core part of the PP extrudate with $R = 30\%$.

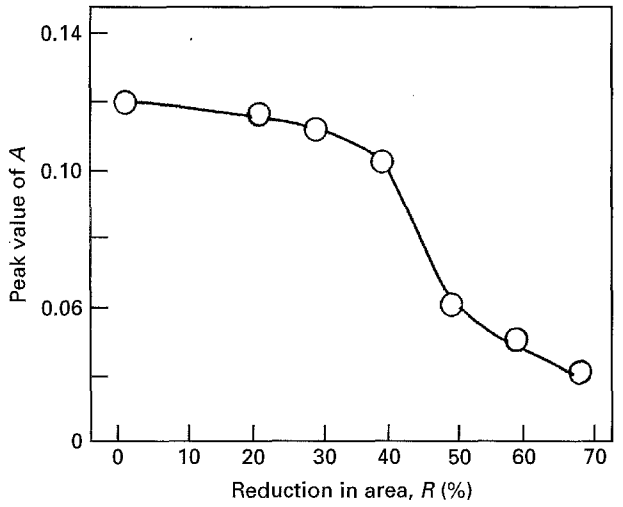

Figure 7 Peak value of A versus reductions in area R.

modulus, G', is inversely proportional to T^2, where T is the time period [24]. The value of this period, therefore, reflects strongly the modulus G' above 0 °C, as shown in Fig. 5. Thus, the bend at about 50 °C in the G' curves of the extrudate with $R = 80\%$ and the cold-drawn sample with draw ratio of $\lambda = 5$ is caused by the length of the period accompanying the molecular change.

3.4. Melting behaviour of thermophotometry (TP) tests

Fig. 8 shows the light transmitting intensity versus temperature for the extrudates perpendicular to the direction of hydrostatic extrusion (or cutting angle of $\theta = \pi/2$ rad). The light transmitting intensity curve shows a small shoulder peak for the extrudates below $R = 50\%$, near the melting point, and a large peak for the extrudates above $R = 50\%$. The large peak for the extrudates above $R = 50\%$ is related to the elliptical structure of the spherulites. In addition, the TP curves of the extrudates above $R = 50\%$ parallel to the direction of hydrostatic extrusion (or a cutting angle of $\theta = 0$ rad) are similar to those of the extrudates at $\theta = \pi/2$ rad [25]. The decrease in the light intensity at about 80 °C is related to the motion of the amorphous region within the spherulites and the further decrease at 150 °C is caused by melting of the spherulites.

It is reported [25] that the intensity curve in the uniaxially extended film with strain $\varepsilon = 0$, is quite different from that in other TP curves with different strains with $\varepsilon = 0.5$, 1, 1.5, 2, and 3: the small peak with strain, $\varepsilon = 0$, observed at about 154 °C is attributed to the melting of β-crystals. This peak is gradually reduced in intensity with increase in strain, ε; this peak disappears in the extended films with $\varepsilon = 1.5$. In the extended films above $\varepsilon = 2$, only a single peak is observed; this peak is attributed to the melting of α-crystals. The resulting behaviour exhibiting a single peak in the extended films, is basically identical to that in the extruded samples. The shape of the TP curve in the extruded sample with $R = 50\%$ is very similar to that in the extended film with $\varepsilon = 1.0$. Because the amount of strain of $\varepsilon = 1.0$ corresponds

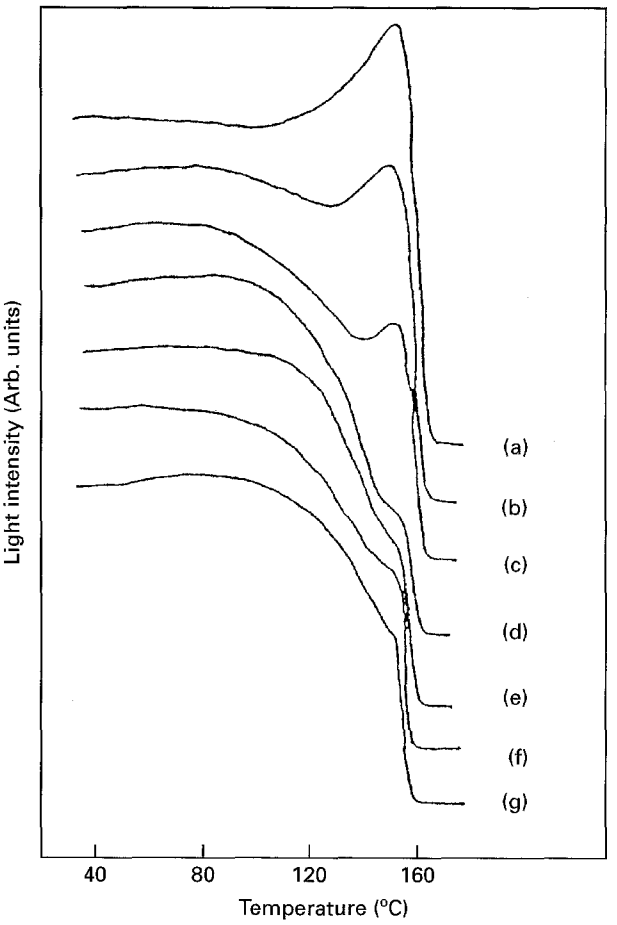

Figure 8 Light intensity versus temperature of PP extrudates with different reductions in area R: (a) 80%; (b) 70%; (c) 60%; (d) 50%; (e) 40%; (f) 30%; (g) virgin sample. Curves are shifted vertically for clarity.

relatively to $R = 50\%$, the amount of $\varepsilon = 1.0$ (or $R = 50\%$) gives a critical number. In fact, the deformation mechanism in the extrudates produced by hydrostatic extrusion was divided in two stages below/above $R = 50\%$. The shape of spherulites changed from spherical to elliptical in the extrudate above $R = 50\%$; the spherulite with $R = 50\%$ changed from coarse structure to a finer one by the imposition of hydrostatic pressure.

Figs 9 and 10 shows the ratio, R_i, of light intensity in the extruded samples at various cutting angles of $\theta = \pi/2$ and 0 rad, respectively, together with the melting temperature, T_{mp}. The melting point, T_{mp}, is defined as the end-off temperature at which the light intensity becomes levelled off (the viewing field of the polarizing microscope becomes dark). R_i is defined as $R_i = I/I_0$; I is the intensity at a peak temperature and I_0 is the intensity at room temperature. R_i at $\theta = \pi/2$ and 0 rad, in the extrudate with $R = 50\%$, is the minimum in all extrudates. R_i at both $\theta = \pi/2$ and 0 rad increases with increasing reduction in area above $R = 50\%$. This behaviour is due to the same morphological change between the molecular chains parallel and perpendicular to the direction of hydrostatic extrusion. On the other hand, R_i in the extended films remained constant at 1.0 at the strain range of $\varepsilon = 0$–1.0 [25]. In addition, R_i in both the samples of the extended film and the extrudate indicated the similar behaviour above $\varepsilon = 1.0$ (or $R = 50\%$); both

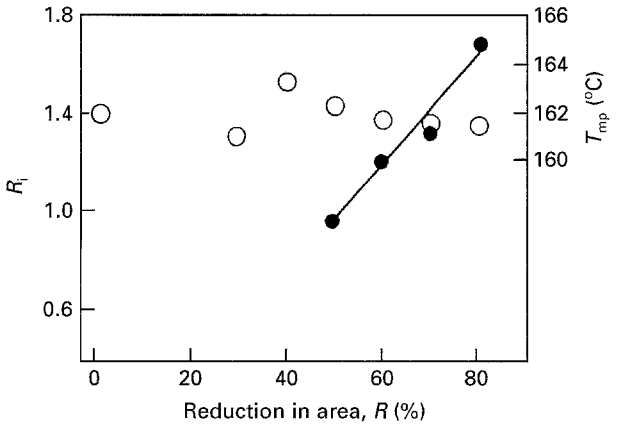

Figure 9 The ratio, R_i, of light intensity (●) and melting point, T_{mp}, (○) versus reduction in area, R, of PP extrudates perpendicular to the direction of hydrostatic extrusion (cutting angle $\theta = \pi/2$ rad).

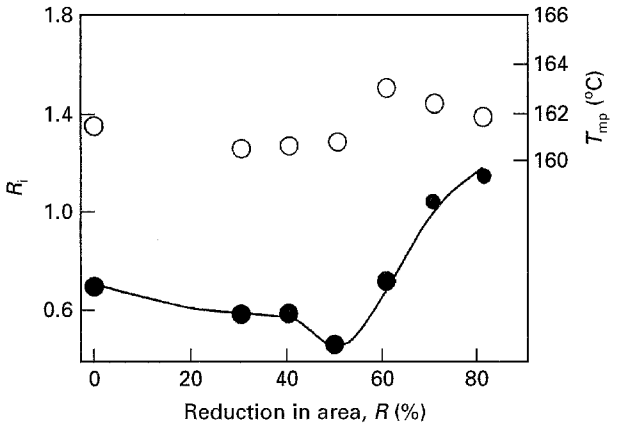

Figure 10 The ratio, R_i, of light intensity (●) and melting point, T_{mp}, (○) versus reduction in area, R, of PP extrudates parallel to the direction of hydrostatic extrusion (cutting angle $\theta = 0$ rad).

R_i increase with increasing strain ε and reduction R. T_{mp} behaviour at both the $\theta = \pi/2$ and 0 rad does not show a significant change, irrespective of little change in the variation of 3 °C. The behaviour of R_i agrees well with that of the size of the spherulite, the melting temperature, T_{mp}, and the specific heat [20, 25].

4. Conclusions

To clarify the change in spherulites for hydrostatically extruded polypropylene (PP), torsional dynamic mechanical properties and the melting behaviour of the PP extrudates have been investigated by the use of internal friction measurements and thermophotometry (TP) tests. The results are discussed on the basis of spherulitic structure. The temperature dependence of tan δ (loss factor) shows that two separate peaks are observed for the virgin sample over the temperature range tested here. In contrast, tan δ curves for the extrudates show complicated features. The onset temperature of the β-loss peak decreases with increasing reduction in area, R.

For the extrudates below $R = 50\%$, both the onset temperature of the β-loss and the peak temperature of the α-loss, shift to lower temperature. For the extrudates above $R = 50\%$, the α absorption shifts to the higher temperature, in contrast to the curve behaviour of the reduction in area below $R = 50\%$. It is noticed that the temperature of the β-loss peaks does not shift and remains constant at 5 °C. The T_g value agrees with the onset temperature of the virgin sample. These β- and α-loss peaks in the virgin sample are clearly separated.

The intensity of the β-loss peak, Δ_{max}, is maximum for the extrudate with $R = 50\%$. The results of tan δ, damping, and the intensity of the β-loss peak indicate that the mechanism of molecular chain deformation is divided into two stages below and above $R = 50\%$. The increase in β-loss peak intensity is due to the increase in amorphous molecules squeezed from the interior of spherulites by hydrostatic extrusion. This is because the location of the onset temperature for the β-loss peak shifts to a lower temperature as the reduction in area increases.

The α absorption for the extrudates above $R = 50\%$ differs from that of the virgin sample: the α-peak temperature for the extrudates is higher by about 20 °C than that for the virgin sample. The overlap of α- and β-losses is due to molecular chains strained on hydrostatic extrusion. The peak value, A, decreases with increasing reduction in area. In particular, the steep decrease in the value A is observed at the reduction in area of $R = 40$–50%. This fact is due to the change of chain deformation. The light transmitting intensity curve shows a small shoulder peak for the extrudates below $R = 50\%$, near the melting point, and a large peak for the extrudates above $R = 50\%$. The large peak for the extrudates above $R = 50\%$ is related to the elliptical structure of spherulites. The decrease in the light intensity at about 80 °C is related to the motion of the amorphous region within spherulites and the further decrease at 150 °C is caused by melting of spherulites.

References

1. K. D. PAE and S. K. BHATEJA, *J. Macromol. Sci. Rev. Macromol. Chem.* **C13** (1975) 1.
2. H. U. D. PUCH and A. H. LOW, *J. Inst. Metals* **93** (1964) 201.
3. L. A. DAVIS, *Polym. Eng. Sci.* **14** (1974) 641.
4. K. IMADA, T. YAMAMOTO, K. SHIGEMATSU and M. TAKAYANAGI, *J. Mater. Sci.* **6** (1971) 537.
5. J. SAUER and K. D. PAE, *Colloid Polym. Sci.* **252** (1974) 680.
6. A. G. GIBSON, I. M. WARD, B. N. COLE and B. PARSONS, *J. Mater. Sci.* **9** (1974) 1193.
7. S. BURGESS and D. GREIG, *J. Phys. C Solid State Phys.* **8** (1975) 1637.
8. K. NAKAYAMA and H. KANETSUNA, *J. Mater. Sci.* **10** (1975) 1105.
9. *Idem, ibid.* **12** (1977) 1477.
10. A. G. GIBSON, D. GREIG, M. SAHTA, I. M. WARD and C. L. CHOY, *J. Polym. Sci. Polym. Lett. Edn.* **15** (1977) 183.
11. J. H. SOUTHERN, N. WEEKS, R. S. PORTER and R. CRYSTAL, *Makromol. Chem.* **162** (1972) 19.
12. N. WEEKS and R. S. PORTER, *J. Polym. Sci. Polym. Phys.* **12** (1974) 635.
13. N. CAPIATI and R. S. PORTER, *ibid.* **13** (1975) 1177.
14. A. BUCKLEY and H. A. LONG, *Polym. Eng. Sci.* **9** (1969) 115.
15. T. WILLIAMS, *J. Mater. Sci.* **8** (1973) 59.
16. H. N. YOON, K. D. PAE and J. SAUER, *Polym. Eng. Sci.* **16** (1976) 567.
17. T. NAKAYAMA and N. INOUE, *Trans. JSME* **42** (1976) 3126.

18. *Idem, Bull. JSME* **20** (1977) 688.
19. K. NAKAYAMA, H. KANETSUNA and E. NODA, *J. Jpn. Soc. Tech. Plast.* **20** (1979) 820.
20. T. ARIYAMA and M. TAKENAGA, *Polym. Eng. Sci.* **31** (1991) 1101.
21. *Idem, ibid.* **34** (1994) 1269.
22. T. ARIYAMA, T. NAKAYAMA and N. INOUE, *J. Polym. Sci. Polym. Lett. Edn.* **15** (1977) 427.
23. T. TSUCHIYA, M. OTONARI and T. ARIYAMA, *J. Ceram. Soc. Jpn* **95** (1987) 267.
24. T. ARIYAMA and M. TAKENAGA, *Polym. Eng. Sci.* **32** (1992) 705.
25. T. ARIYAMA, *J. Mater. Sci.* **27** (1992) 4940.
26. G. FARROW, *Polymer* **2** (1960) 409.
27. N. INOUE, T. NAKAYAMA and T. ARIYAMA, *J. Macromol. Sci. Phys.* **B19** (1981) 543.
28. P. MANARESI and V. GANNELLA, *J. Appl. Polym. Sci.* **4** (1960) 251.
29. D. R. MEARS, K. D. PAE and J. A. SAUER, *J. Appl. Phys.* **40** (1969) 4229.
30. G. JOURDAN, J. Y. CAVILLE and J. PEREZ, *J. Polym. Sci. Part B* **27** (1989) 2361.

Received 22 December 1994
and accepted 13 February 1996